

# Broadening the Utility of Farnesyltransferase-Catalyzed Protein Labeling Using Norbornene–Tetrazine Click Chemistry

Shelby A. Auger, Sneha Venkatachalapathy, Kiall Francis G. Suazo, Yiao Wang, Alexander W. Sarkis, Kaitlyn Bernhagen, Katarzyna Justyna, Jonas V. Schaefer, James W. Wollack, Andreas Plückthun, Ling Li, and Mark D. Distefano\*



Cite This: <https://doi.org/10.1021/acs.bioconjchem.4c00072>



Read Online

ACCESS |



Metrics & More

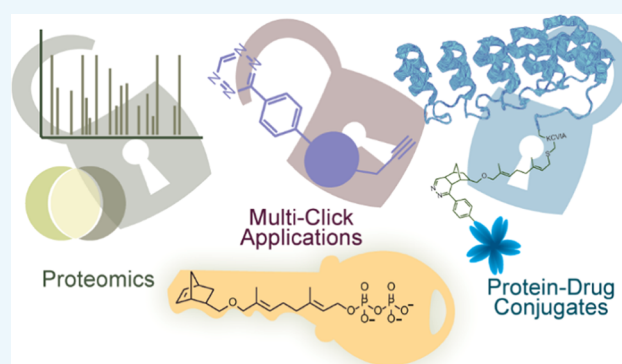


Article Recommendations



Supporting Information

**ABSTRACT:** Bioorthogonal chemistry has gained widespread use in the study of many biological systems of interest, including protein prenylation. Prenylation is a post-translational modification, in which one or two 15- or 20-carbon isoprenoid chains are transferred onto cysteine residues near the C-terminus of a target protein. The three main enzymes—protein farnesyltransferase (FTase), geranylgeranyl transferase I (GGTase I), and geranylgeranyl transferase II (GGTase II)—that catalyze this process have been shown to tolerate numerous structural modifications in the isoprenoid substrate. This feature has previously been exploited to transfer an array of farnesyl diphosphate analogues with a range of functionalities, including an alkyne-containing analogue for copper-catalyzed bioconjugation reactions. Reported here is the synthesis of an analogue of the isoprenoid substrate embedded with norbornene functionality (C10NorOPP) that can be used for an array of applications, ranging from metabolic labeling to selective protein modification. The probe was synthesized in seven steps with an overall yield of 7% and underwent an inverse electron demand Diels–Alder (IEDDA) reaction with tetrazine-containing tags, allowing for copper-free labeling of proteins. The use of C10NorOPP for the study of prenylation was explored in the metabolic labeling of prenylated proteins in HeLa, COS-7, and astrocyte cells. Furthermore, in HeLa cells, these modified prenylated proteins were identified and quantified using label-free quantification (LFQ) proteomics with 25 enriched prenylated proteins. Additionally, the unique chemistry of C10NorOPP was utilized for the construction of a multiprotein–polymer conjugate for the targeted labeling of cancer cells. That construct was prepared using a combination of norbornene–tetrazine conjugation and azide–alkyne cycloaddition, highlighting the utility of the additional degree of orthogonality for the facile assembly of new protein conjugates with novel structures and functions.



## INTRODUCTION

Chemical probes infixed with bioorthogonal functionality have become particularly important tools for the study of biological processes. Such probes are used for substrate identification, site-selective modification, or to give insights into enzyme function. Bioorthogonal probes have been highly useful in the study of protein prenylation, a post-translational modification involved in cellular signaling and regulation. Dysregulation of prenylation has been implicated in several diseases, including cancer, Alzheimer's disease (AD), malaria, and progeria.<sup>1–6</sup> During prenylation, either farnesyl or geranylgeranyl groups (Figure 1A) from the corresponding diphosphates (farnesyl diphosphate (FPP) and geranylgeranyl diphosphate (GGPP), respectively) are transferred onto a cysteine present in a distinctive C-terminal amino acid motif. That motif is typically CaaX, CCXX, CXC, or CC, where C is the site of modification (a cysteine residue), a is generally an aliphatic amino acid, and X is a variable amino acid.<sup>3,7</sup> The specific sequence determines whether the protein is a substrate for farnesyltransferase

(FTase), geranylgeranyl transferase I (GGTase I), geranylgeranyl transferase II (GGTase II), or geranylgeranyl transferase III (GGTase III) (Figure 1B).<sup>8,9</sup> The enzymes that catalyze prenylation have demonstrated structural flexibility regarding their isoprenoid substrate.<sup>10–13</sup> This allows for the transfer of FPP analogues with bioorthogonal functionalities to putative prenylated proteins for site-specific modification, visualization, or drug delivery.

Previous work on prenyltransferases has focused on the transfer of alkyne-functionalized isoprenoids, such as C15AlkOPP (Figure 1A), to prenylated proteins for labeling with azide-containing reagents through copper-catalyzed azide–alkyne

Received: February 20, 2024

Revised: April 12, 2024

Accepted: April 12, 2024

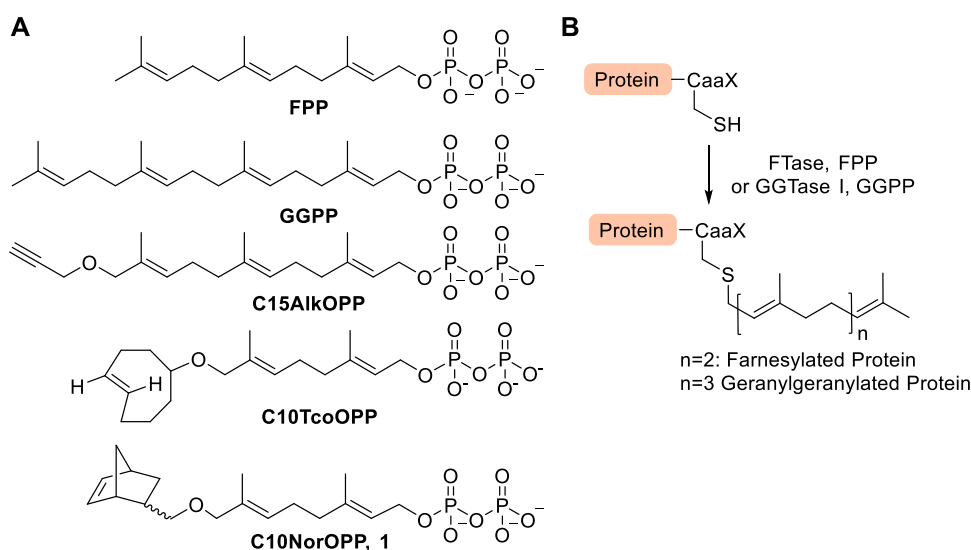


**Figure 1.** Isoprenoids and the reactions using them catalyzed by prenyltransferases. (A) The structures of the natural substrates farnesyl diphosphate (FPP) and geranylgeranyl diphosphate (GGPP). The structures of the well-studied C15AlkOPP analogue and a previously reported analogue of FPP-capable tetrazine ligation, C10TcoOPP, and the norbornene-modified analogue (C10NorOPP, **1**) developed here are also shown. (B) Prenylation reaction catalyzed by farnesyltransferase and geranylgeranyl transferase type I. Note: Compound **1** is a mixture of inseparable diastereomers indicated by the wavy bond. The diastereomers can be distinguished in  $^1\text{H}$  NMR with the *endo* diastereomer designated as **1a** and the *exo* diastereomer as **1b**. That 8:2 mixture of the two is designated as **1** throughout the manuscript.

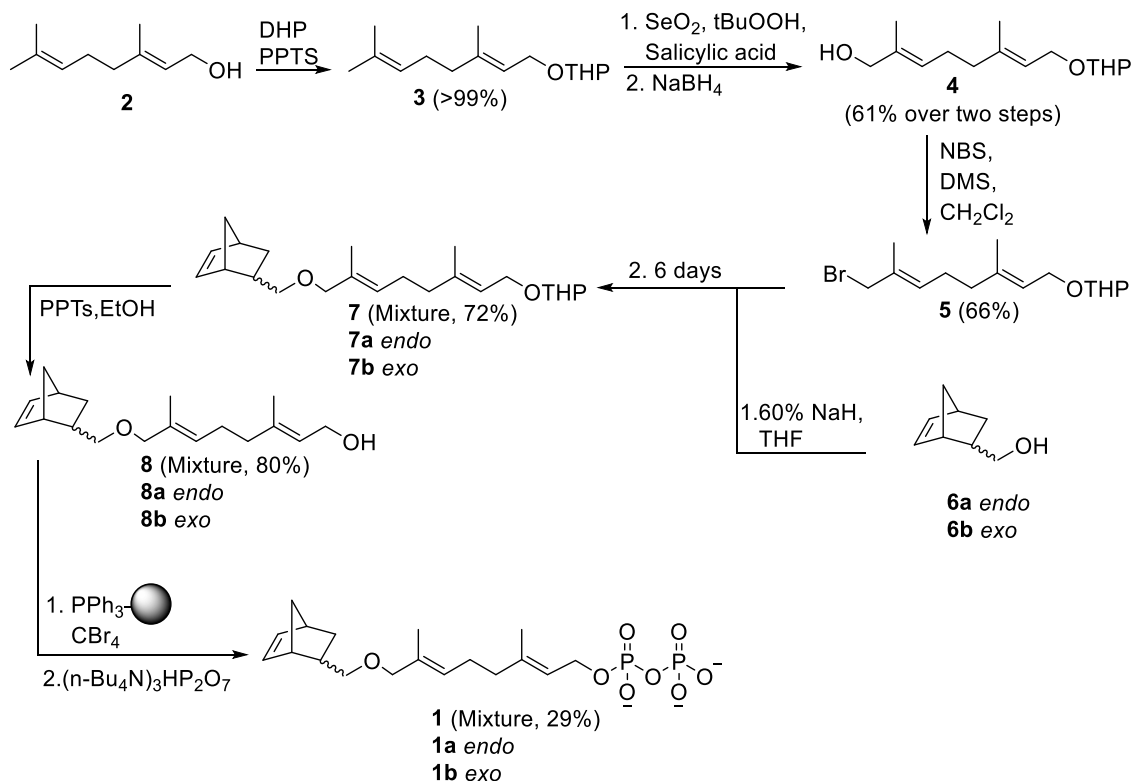
cycloaddition (CuAAC).<sup>13–15</sup> While CuAAC is the most prevalent bioorthogonal labeling strategy, there are many other types of bioorthogonal labeling reactions. Those include the strain-promoted azide–alkyne cycloaddition (SPAAC) or inverse electron demand Diels–Alder (IEDDA) reaction, both of which provide alternative bioorthogonal chemistry for protein modification.<sup>16–19</sup> In previous work, a *trans*-cyclooctene (TCO)-containing FPP analogue (C10TcoOPP) capable of undergoing an IEDDA reaction with a tetrazine-containing tag was reported.<sup>20</sup> While C10TcoOPP demonstrated full ligation with a tetrazine in as little as 15 min, the TCO moiety is synthetically difficult to produce and the large hydrophobic group is too large to be efficiently processed by the enzyme. Other cyclic alkenes, such as cyclopropene ( $k_2 = 4.5 \times 10^2 \text{ M}^{-1} \text{ s}^{-1}$  at 20 °C) or norbornene ( $k_2 = 10 \text{ M}^{-1} \text{ s}^{-1}$  at 20 °C), manifest reactivities with tetrazine slower than TCO ( $k_2 = 1.3 \times 10^4 \text{ M}^{-1} \text{ s}^{-1}$ ) but have been shown to be effective for various in cellulo labeling applications.<sup>16,17,21</sup>

It has been previously demonstrated that probes such as C15AlkOPP can serve as substrates for endogenous prenyltransferases to generate prenylated proteins, incorporating bioorthogonal alkyne moieties via metabolic labeling. Using CuAAC technology, these modified proteins can then be visualized in-gel to elucidate the levels of prenylation or enriched via biotin pull-down for subsequent proteomic analysis to identify specific prenylated proteins. This methodology using C15AlkOPP and related alkyne probes has enabled the identification of many prenylated proteins and variations in their levels to be tracked in disease.<sup>15,22,23</sup> However, it is likely that the existing probes do not capture the entire prenylome. Previous work suggests that the position of the bioorthogonal group within an isoprenoid structure impacts the efficiency of its incorporation. Hence, it is quite possible that changing the structure of the bioorthogonal group will also affect the incorporation efficiency and may reveal new prenylated proteins.

Furthermore, the development of prenylation as a tool for selective protein modification is a burgeoning field. In the past, analogues of FPP capable of SPAAC or CuAAC have been employed for the creation of protein conjugates that can be used for selective visualization of cancer cells.<sup>24–26</sup> The assembly of protein–drug conjugates that link functional proteins with small molecules, including fluorescent dyes and drugs, has proven to be valuable for diagnostic and therapeutic purposes.<sup>27–29</sup> Bioorthogonal chemistry is particularly useful for generating protein conjugates because it allows modification to occur at a specific position on the protein, which leads to the production of homogeneous conjugates with a uniform structural composition. In earlier work, site-specifically labeled protein conjugates obtained by prenylating Designed Ankyrin Repeat Proteins (DARPs)<sup>30,31</sup> with different orthogonal probes allowed selective labeling and killing of cancer cells. While, in the past, different azide–alkyne strategies have been used, combining these two strategies to form more complex conjugates can be difficult due to cross-reactivity. However, combining an IEDDA probe with established azide/alkyne chemistry eliminates this cross-reactivity issue.

Reported here is the synthesis and application of an FPP analogue, incorporating a norbornene moiety (C10NorOPP, **1** Figure 1A) for the study of prenylation. This new FPP analogue is a useful addition to the toolbox of bioorthogonal isoprenoid substrate analogues since it is smaller in size and more stable than TCO, which facilitates a number of new biological applications. Initial *in vitro* enzymatic assays indicated that C10NorOPP could serve as a potentially useful probe by metabolic incorporation into cells and subsequent in-gel fluorescence and label-free chemical proteomic analyses. Additionally, the synchronous application of complementary IEDDA and CuAAC labeling strategies allowed for the creation of new multifunctional protein–drug conjugates. This broad utility makes C10NorOPP a useful multi-tool for both direct investigation of protein prenylation and the development of prenylation-based therapeutic agents.

Scheme 1. Synthesis of C10NorOPP, 1, from Geraniol over Seven Steps



## RESULTS AND DISCUSSION

**Docking Analysis of a Norbornene Analogue into the Active Site of Farnesyltransferase.** To gain insight into whether a norbornene-containing analogue of FPP could be accommodated into the active site of farnesyltransferase, both the *endo* (1a) and *exo* (1b) diastereomers of compound C10NorOPP were docked into the active site of rat FTase (rFTase). Inspection of the docked structures superimposed onto the natural substrate FPP bound to the enzyme shows very good alignment of the diphosphate moieties and the first isoprene units. The conformation of the second isoprene unit in 1a closely tracks that of FPP, while 1b exhibits a significant rotation of nearly 180° of the C-7 methyl group. Interestingly, the norbornene group in 1a does not extend past the terminal carbon (C-12) of FPP, while in 1b, it extends modestly (1.7 Å) beyond that point. These observations indicate that C10NorOPP can be readily accommodated into the rFTase active site and suggest that it can act as an effective FPP surrogate.

**Synthesis of C10NorOPP (1).** The synthesis of C10NorOPP was completed in seven steps from commercially available geraniol (2) (Scheme 1). Alcohol 4 was prepared as previously reported.<sup>13</sup> Bromide 5 was synthesized by allylic bromination of compound 4 using *N*-bromosuccinimide and dimethylsulfide. A mixture of *endo* (6a) and *exo* (6b) 5-norbornene-2-methanol was deprotonated with NaH, followed by the addition of alkyl halide 5 to give the ether-linked norbornene isoprenoid 7.

Deprotection of that species gave alcohol 8, and its subsequent activation to the corresponding bromide allowed the incorporation of a diphosphate moiety to yield the target compound, 1, in 7% overall yield over seven steps (Scheme 1). It should be noted that since compound 6 was an inseparable 4:1 diastereomeric mixture of *endo* (6a) and *exo* (6b)

stereoisomers, compounds 7, 8, and 1 are all mixtures of *endo* (7a, 8a, and 1a) and *exo* (7b, 8b, and 1b) isomers, with the *endo* isomers present as the main components (~80%). This was confirmed via <sup>1</sup>H NMR spectroscopy of 7, 8, and 1. For example, in the <sup>1</sup>H-analysis of 7 (Figure S1), the ratio of the *endo*/*exo* isomers was 82:18. This ratio was determined by comparing the integration for the *endo* hydrogen peak at 6.14 ppm with the smaller *exo* signal at 6.07 ppm. <sup>1</sup>H NMR analysis of 8 and 1 revealed a similar ratio (Figure S1). Since 1a and 1b were not separable, that mixture is referred to as C10NorOPP (1). While identification of both the *endo* and *exo* components was important for the characterization of the above compounds, the presence of this mixture was not deemed to be a significant concern for subsequent applications since the *endo* and *exo* norbornene moieties are known to undergo tetrazine ligation at similar rates, although it is worth noting that the *exo* isomer of norbornene-containing compounds does react modestly (~3-fold) faster.<sup>21,32</sup> Conversely, based on the aforementioned docking experiments (Figure 2), *endo* 1a appears to manifest fewer conformational differences (relative to FPP) compared with *exo* 1b and binds in a conformation that is more similar in length to FPP, suggesting that 1a may be a more efficient substrate for farnesyltransferase.

**Analysis of C10NorOPP as a Substrate for FTase.** While it was expected that C10NorOPP would be a suitable alternative substrate for farnesyltransferase, given previous results with other probes with moieties of a similar size such as 1 and others,<sup>33</sup> it was still necessary to establish whether C10NorOPP was efficiently incorporated by the enzyme. To accomplish that, an *in vitro* prenylation reaction using yeast farnesyltransferase (yFTase) and the well-characterized peptide substrate, *N*-dansyl-GCVIA (DsGCVIA, 9), was analyzed via liquid chromatography-mass spectrometry (LC-MS). It is important to note that while initial docking experiments were

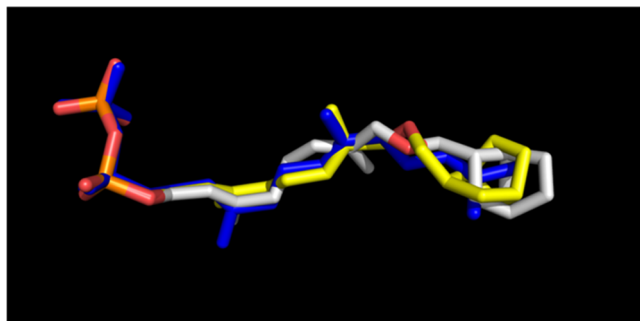


**Figure 2.** Conformations of **1a** (*endo*) and **1b** (*exo*) docked into the active site of rFTase. Compounds **1a** and **1b** are superimposed on the physiological ligand FPP. The protein structure (JCR) is omitted for clarity. FPP: blue; **1a**: carbon (yellow), oxygen (red), and phosphorus (orange); **1b**: carbon (white), oxygen (red) and phosphorus (orange).

carried out using rFTase, the kinetic parameters and enzymatic tests were performed with yFTase. This was performed because yFTase is a more efficient enzyme and hence is more suitable for enzymatic protein modification; therefore, determining these parameters for yFTase and the specific CaaX sequence used in the protein constructs is more useful on a practical level. Unfortunately, there is no X-ray structure of yFTase. Although there is only a 39 and 29% sequence identity between rFTase and yFTase for their  $\beta$  and  $\alpha$  subunits, respectively, both have the capabilities to transfer bioorthogonal probes.<sup>34,35</sup>

Inspection of the chromatogram (Figure S2) revealed a change in the retention time between the norbornene-modified product (DsGC[Nor]VIA (**10**),  $r_t = 13.9$  min) and unmodified DsGCVIA ( $r_t = 5.99$  min, **9**), resulting from increased hydrophobicity due to the addition of the modified isoprenoid. The  $m/z$  value of the later-eluting product was also consistent with the formation of the expected product (**10**: calcd  $[M + 2H]^{2+} = 477.1$ ; found  $[M + 2H]^{2+} = 477.2$ ). To investigate whether DsGC[Nor]VIA, **10**, retained reactivity for the reaction, the modified peptide was purified and reacted with benzyl amino tetrazine, **11**, for 2 h. Analysis by LC-MS analysis showed a mixture of unreacted DsGC[Nor]VIA ( $r_t = 13.9$  min) and the desired tetrazine-modified product (DsGC[Nor-Tet]VIA, **12**,  $r_t = 8.24$  min; calcd  $[M + 3H]^{3+} = 371.2$ , found  $[M + 3H]^{3+} = 371.5$ ), confirming that the transfer to peptide **10** did not hinder the iEDDA reaction between the norbornene and tetrazine.

After the confirmation that C10NorOPP was a viable substrate for yFTase, a continuous spectrofluorimetric activity assay was used to measure the prenylation rate using C10NorOPP and **10** as substrates. This assay has been used extensively to determine kinetic constants for a variety of FPP analogues, including C15AlkOPP and C10TcoOPP, and it relies on the increase in dansyl group fluorescence that occurs when its environment becomes less polar due to the covalent attachment of hydrophobic isoprenoid moieties. Direct curve fitting of the plot (Figure S3) of rate versus the concentration of C10NorOPP using the Michaelis–Menten equation yielded values for  $K_M$  ( $0.88 \mu\text{M}$ ) and  $k_{\text{cat}}$  ( $4.6 \text{ s}^{-1}$ ) that were similar to those obtained for FPP (Table 1). Overall, the catalytic efficiency obtained using C10NorOPP was  $\sim 2$ -fold higher than that observed with FPP. In contrast, a comparison of C10NorOPP with C10TcoOPP showed that while they both manifested comparable  $K_M$  values, the  $k_{\text{cat}}$  value for the former

**Table 1.** Kinetic Values for the yFTase-Catalyzed Reaction between DsGCVIA and C10TcoOPP, C10NorOPP, or FPP

	$K_M$ ( $\mu\text{M}$ )	$k_{\text{cat}}$ ( $\text{s}^{-1}$ )	rel $k_{\text{cat}}$	$\frac{k_{\text{cat}}}{K_M}$ ( $\mu\text{M}^{-1} \text{ s}^{-1}$ )
FPP <sup>a</sup>	$0.76 \pm 0.03$	$2.2 \pm 0.1$	1	$2.9 \pm 0.1$
C10NorOPP, <b>1</b> <sup>a</sup>	$0.88 \pm 0.03$	$4.6 \pm 0.3$	2.1	$5.2 \pm 0.4$
C10TcoOPP <sup>b</sup>	0.77	0.1	0.05	0.13

<sup>a</sup>All values are presented for FPP and **1**, which are apparent kinetic parameters since they were determined at a single peptide concentration ( $2.4 \mu\text{M}$ ). The values reported are the averages and standard deviations from three separate replicates. <sup>b</sup>The results for C10TcoOPP were previously reported and were determined using  $5 \mu\text{M}$  peptide.<sup>20</sup>

( $4.6 \text{ s}^{-1}$ ) was dramatically (46-fold) higher than that of the latter ( $0.1 \text{ s}^{-1}$ ). This observation is particularly important since it suggests that C10NorOPP should be effective at labeling protein substrates inside cells, where endogenous FPP is also present, in contrast to C10TcoOPP, which reacts  $\sim 40$ -fold slower. Thus, C10NorOPP represents a considerable improvement in the design of bioorthogonal FTase substrates.

To study whether C10NorOPP could serve as an effective FTase substrate in a more biologically relevant context, labeling experiments with TAMRA-PEG4-tetrazine (TAMRA-tetrazine, **13**) were performed with *in vitro* prenylation reactions carried out in HeLa cell lysates. In this experiment, HeLa cells were pretreated with lovastatin, **14**, an HMG-CoA reductase inhibitor that decreases the endogenous levels of FPP and GGPP, in order to provide a pool of unprenylated proteins that could then be labeled using C10NorOPP in a subsequent *in vitro* prenylation reaction.

Cell lysates were then treated with C10NorOPP and yFTase or rFTase in the presence of exogenously added GFP-CVIA, a well-established full-length protein substrate.

The samples were treated with tetrazine-TAMRA, compound **13**, and analyzed by in-gel fluorescence (Figure 3). This demonstrated that GFP-CVIA could be modified with C10NorOPP by both yFTase and rFTase and be labeled with **13**, as indicated by the intense band at  $\sim 30$  kDa (Figure 3, lanes 4 and 8). While there was some background fluorescence observed in the absence of C10NorOPP (Figure 3, lanes 1 and 5), additional labeling of endogenous prenylated proteins was observed in the reactions containing C10NorOPP, as evidenced by the increase in intensity of at least one band in the 50 kDa region (Figure 3, lanes 2 and 4, highlighted with an arrow). Taken together, these experiments demonstrate that both full-length endogenous cellular proteins and exogenously added proteins can be successfully prenylated with C10NorOPP.

**Metabolic Labeling and Prenylomic Analysis with C10NorOPP.** Since the experiments established that full-length protein substrates could be labeled *in vitro* using C10NorOPP, subsequent experiments focused on whether C10NorOPP could be incorporated *in cellulo* via metabolic labeling procedures. Previous work has shown that alkyne- and azide-containing isoprenoid analogues can be incorporated into prenylated proteins using the endogenous prenylation machinery.<sup>10,11,15,36</sup> Here, metabolic incorporation was studied in HeLa, COS-7, and immortalized astrocyte cells since these cell lines have been previously studied with alkyne-based probes and shown to manifest different levels of probe incorporation.<sup>14</sup> Accordingly, these cell lines were subjected to

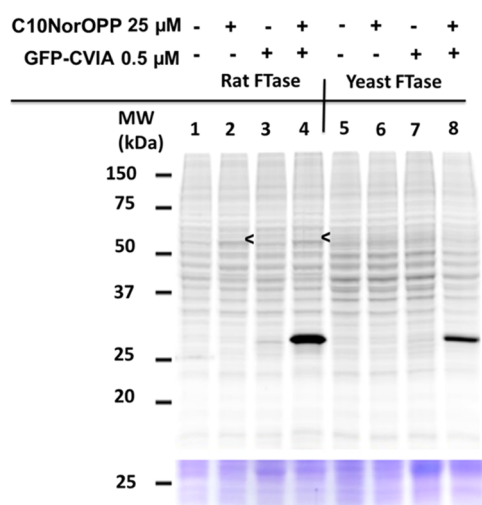


**Figure 3.** *In vitro* prenylation reaction in HeLa cell lysate supplemented with exogenously produced GFP-CVIA. HeLa cell lysate was treated with rFTase or yFTase and supplemented with C10NorOPP or GFP-CVIA. The CVIA modification allows GFP to be prenylated by the FTase enzymes. The top panel shows TAMRA fluorescence, and the bottom panel shows a portion of the Coomassie blue stained gel. Lanes 1–4 were treated with rFTase and lanes 5–8 were treated with yFTase. Lanes 1 and 5 are the respective controls treated with neither GFP-CVIA nor C10NorOPP. Lanes 2 and 6 were treated with C10NorOPP, lanes 3 and 7 were treated with GFP-CVIA, and lanes 4 and 8 were treated with both GFP-CVIA and C10NorOPP. All samples were subjected to tetrazine ligation for 3 h with TAMRA-tetrazine 13.

metabolic labeling with C10NorOPP followed by in-gel fluorescence (Figure 4A).

In this process, cells were either pretreated with or without lovastatin prior to incubation with C10NorOPP for 24 h.<sup>37</sup> After treatment with C10NorOPP, the cells were lysed and the crude lysate was subjected to an *in vitro* iEDDA click reaction with TAMRA-tetrazine and then analyzed via in-gel fluorescence. In all three cell types (Figure 4B–D), it was observed that lovastatin pretreatment (lane 3 in Figure 4B,D, lane 4 in Figure 4C) followed by treatment with C10NorOPP showed substantially more labeling compared to treatment with C10NorOPP alone (Figure S4).

To confirm that the proteins being labeled were in fact putative prenylated proteins, HeLa cells were co-treated with either FPP or an FTase inhibitor (FTI, L-744,834, 15). Co-treatment with exogenous FPP and C10NorOPP showed diminished labeling (Figure 4B, lane 3) comparable to the control sample, which is consistent with the idea that C10NorOPP is added to otherwise prenylated proteins within cells since the inclusion of the physiological substrate (FPP) should competitively reduce labeling by C10NorOPP. This was further confirmed through an inhibition assay during which the cells were treated with C10NorOPP and an FTI (Figure 4B, lane 4), which also resulted in a decrease in labeling to background levels. This latter result is consistent with specific labeling of farnesylated proteins by C10NorOPP catalyzed by rFTase since 15 is a highly selective inhibitor of that enzyme. Overall, when looking at the no-probe controls in all gels (lanes 1 and 2 in Figure 4B, and lanes 1 in Figure 4C,D), there is significant background fluorescence. This is more than what has been seen with the previously reported azide–alkyne cycloaddition strategies, likely due to non-

specific labeling by the tetrazine moiety or as a result of the 2-fold increased amount of the fluorescent reagent used compared to what is used with the alkyne analogues.

The development of proteomic methods to comprehensively identify the prenylome has relied on the use of bioorthogonal probes for protein enrichment. While prenylomic analysis using substrates containing bioorthogonal functionality has limitations, it remains the most widely used method in the field for characterizing the prenylome in a comprehensive manner.<sup>14,15</sup> Other methods focused on enrichment of prenylated proteins without metabolic labeling are being developed but have not been widely used to date.<sup>38–40</sup> Using alkyne-containing isoprenoid analogues followed by conjugation with biotin-azide allows proteins modified through metabolic labeling to be isolated via avidin enrichment. After confirming that C10NorOPP could be used to metabolically label protein targets of prenylation, chemical proteomics was used to identify which prenylated proteins were modified by C10NorOPP using the workflow shown in Figure 4A. HeLa cells pretreated with lovastatin, 14, were then treated with C10NorOPP or FPP control for 24 h. Three replicates of each of these samples were prepared, lysed, and subjected to an *in vitro* iEDDA click reaction with biotin-PEG4-tetrazine (biotin-tetrazine, 16) and enriched via avidin pull-down. The enriched prenylated proteins were digested with trypsin for a bottom-up proteomic analysis, employing liquid chromatography with tandem mass spectrometry (LC-MS/MS). Using label-free quantification (LFQ), 2790 proteins were identified. These proteins were ranked by increasing fold changes, and proteins with a Log<sub>2</sub> fold change >1 are enriched with C10NorOPP (Figure 5A). Of the 95 proteins that meet that criteria, there are 25 enriched prenylated proteins that were identified, including 11 farnesylated proteins, 8 geranylgeranylated Rab proteins, and 6 geranylgeranylated proteins (Table S1). The number of prenylated proteins is comparable to the number reported in a recent study, describing the prenylomic analysis of HeLa cells treated with C15AlkOPP (Figure 5B), where 29 prenylated proteins were reported.<sup>14</sup>

While the total number of prenylated proteins identified is comparable between C10NorOPP and C15AlkOPP, the identities of the enriched prenylated proteins differ. Interestingly, when comparing the three types of prenylated proteins, farnesylated proteins were the predominant ones identified in the current study, with five distinct farnesylated proteins identified in this work that were not found with the C15AlkOPP analysis in HeLa (Figure S5). Additionally, there are four prenylated Rab proteins and two geranylgeranylated proteins that were also found with C10NorOPP and not with C15AlkOPP in HeLa (Figure S5B,C). Interestingly, when comparing the Log<sub>2</sub> fold changes for the 17 proteins that were found in both experiments, there was no correlation between the fold changes of the proteins found with both probes (Figure 5C). This fact, combined with the variation in the proteins identified with each probe, suggests that C10NorOPP is better suited to label a different subset of prenylated proteins than C15AlkOPP. This is likely because of two reasons. First, it reflects the fact that C10NorOPP is closer in length to FPP than GGPP (Figure 1A). Thus, it is probably not an effective substrate for GGTTases and this is consistent with the observation that C10NorOPP identified fewer geranylgeranylated proteins of both types; in contrast, C15AlkOPP is intermediate in length between FPP and GGPP and has been shown to be efficiently used by all protein

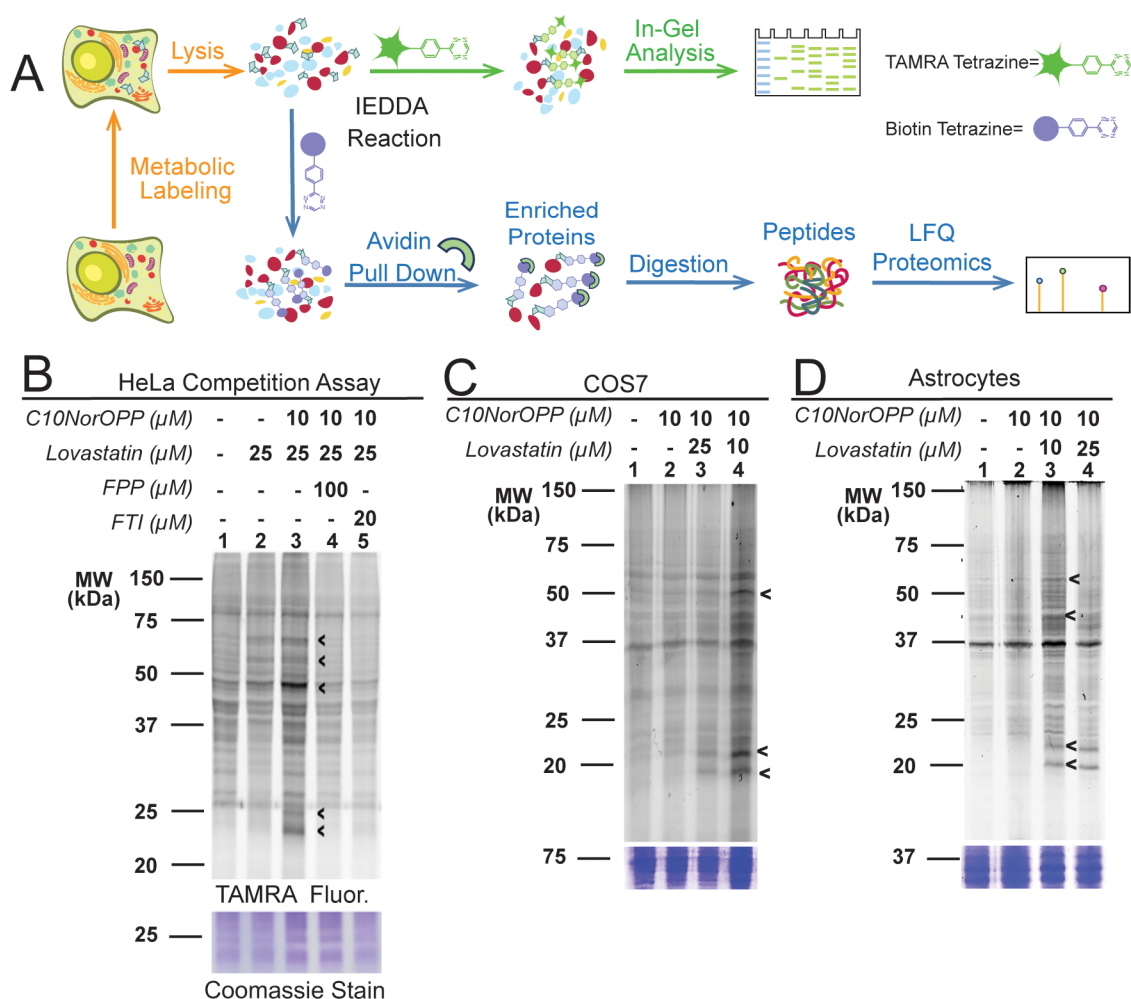


**Figure 4.** Metabolic labeling with C10NorOPP showed consistent labeling of prenylated proteins in several mammalian cell lines. (A) Scheme of metabolic labeling and proteomic workflows showing either an iEDDA click reaction with TAMRA-tetrazine (green) for in-gel fluorescence analysis or an iEDDA click reaction with biotin-tetrazine (16) for prenylomic sample preparation and analysis (blue). (B) In-gel fluorescence analysis of the incorporation of C10NorOPP into HeLa cells and competition analysis with FPP and an FTase inhibitor (FTI, 15). HeLa cells were treated with lovastatin 6 h before 24 h treatment with C10NorOPP, followed by cell lysis and reaction with TAMRA-tetrazine. Top panel: Probe incorporation visualized with TAMRA fluorescence (TAMRA Fluor.); bottom panel: total protein loading, as visualized by Coomassie staining. Arrows in lane 3 highlight proteins labeled with C10NorOPP. (C) In-gel analysis of COS-7 cells and (D) immortalized astrocytes treated as described for HeLa cells. Fluorescence intensities normalized to protein loading for all three gels are plotted in Figure S4.

prenyltransferases.<sup>34</sup> Second, the size of the bioorthogonal handle differs between that of the bicyclic norbornene in C10NorOPP and that of the smaller alkyne in C15AlkOPP, which changes how the probes interact with the protein substrate in the binding pocket of the enzyme. This is revealed when examining the CaaX sequences of the protein substrates found with each probe (Figure 5D,E).

When examining the CaaX sequences identified with only C10NorOPP, there is less variability compared to those found only with C15AlkOPP. Furthermore, the C10NorOPP probe labels proteins with slightly smaller aliphatic residues (Figure 5D). Furthermore, upon examining the more complex modification site in Rab proteins found with either probe (Figure S6C–F), there were more subtle differences, primarily with regard to cysteine placement within the five C-terminal residues. While C10NorOPP primarily labels Rab proteins, where the enzymatically modified cysteines are the two C-terminal residues, C15AlkOPP modifies Rab proteins with no preference for the location of the cysteines (Figure S6D). This observation underscores the fact that subtle differences in the

binding of prenyl analogues to the target enzymes can lead to differences in their incorporation rate, depending on specific features of the enzyme–protein–isoprenoid complex. It is worth noting that in the prenyltransferase ternary complexes (enzyme with the peptide substrate and FPP analogue), numerous atoms from the isoprenoid–donor and peptide–receiver substrates are in direct contact.<sup>43</sup> In earlier work with C15AlkOPP, it was observed in docking experiments that introduction of the alkyne moiety alters the isoprenoid/peptide interface, suggesting that it may alter peptide specificity.<sup>35</sup> That was confirmed experimentally with a series of analogues, incorporating alkyne groups at different positions, each showing a unique pattern of reactivity.<sup>44</sup> Docking experiments with C10NorOPP again show numerous contacts between the analogue and the peptide substrate that likely impact peptide substrate selectivity (Figure S7). It has been previously suggested that employing multiple structurally varied probes in metabolic labeling experiments may be a way to increase the number of experimentally verified prenylated proteins.<sup>44</sup> Our results are consistent with that hypothesis and illustrate how

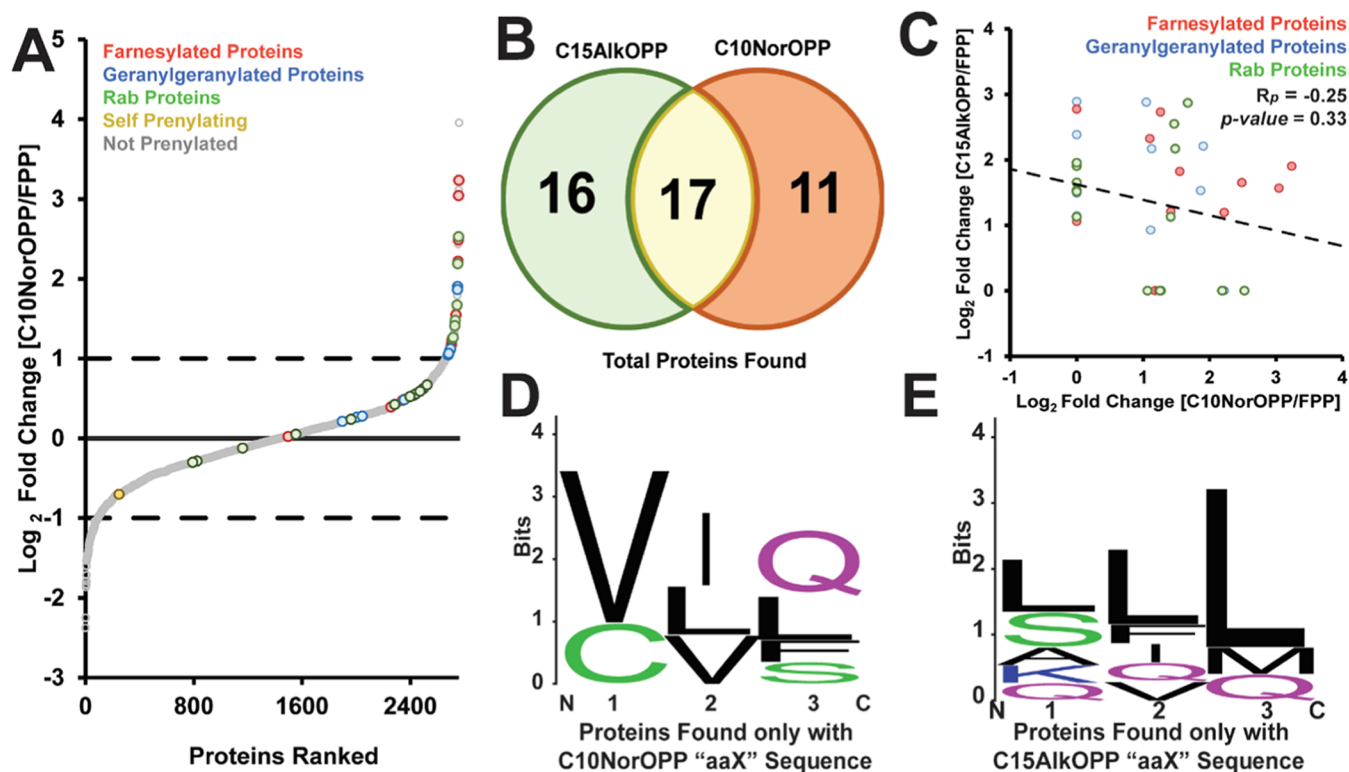


**Figure 5.** Proteomic results and analysis of prenylated proteins found with C10NorOPP. (A) All 2790 proteins found in LFQ prenylomics were ranked from smallest to largest by the  $\text{Log}_2$  fold change [C10NorOPP/FPP]. Proteins with a  $\text{Log}_2$  fold change  $>1$  are significantly enriched in the sample treated with C10NorOPP. Of these 95 proteins, 25 are known to be prenylated. There were additional 21 prenylated proteins that did not meet the cutoff. Red: farnesylated protein substrates, blue: geranylgeranylated type I protein substrates, green: Rab proteins, yellow: ALDH9A1, autoprenylated protein, and gray: proteins not known to be prenylated. (B) Venn diagram comparing ungrouped enriched proteins found with C10NorOPP and previously reported prenylated proteins found with C15AlkOPP in HeLa cells. (C) Pearson correlation plot comparing the fold changes of the 17 proteins found in both C10NorOPP and C15AlkOPP prenylomic profiling of HeLa Cells. (D, E) Sequence logos exploring the differences in the prenylation site of proteins labeled with C15AlkOPP or C10NorOPP. FTase and GGTase I substrates were analyzed separately from GGTase II substrates (Rab proteins, Figure S6). Sequence logos were generated with the web logo tool (<https://weblogo.berkeley.edu/logo.cgi>).<sup>41,42</sup> Prenylated cysteine residues were not included in “CaaX” analysis. Comparison of the “aaX” residues in proteins found with (D) C15AlkOPP (eight proteins) or (E) C10NorOPP (seven proteins).

the use of norbornene-containing analogues and the iEDDA click reaction can be a complementary strategy for exploration of the prenylome.

**Labeling of Epithelial Cell Adhesion Molecule (EpCAM)-Expressing Cancer Cell Lines Using Prenylated DARPin.** Beyond their use in characterizing prenylated proteins, isoprenoid analogues have also proven to be useful for the development of protein-drug conjugates. This is due to the small tetrapeptide CaaX-box motif recognized by FTase that can be appended to virtually any protein, converting it into a prenyltransferase substrate. Using an isoprenoid analogue incorporating bioorthogonal functionality, this strategy can be employed to create a plethora of modified proteins for a variety of applications. To investigate whether C10NorOPP could be used to construct site-specific protein–fluorophore conjugates for targeted cancer cell imaging, an anti-EpCAM Ac2-KCVIA DARPin<sup>45</sup> (D1, 17) engineered to contain a C-terminal CVIA sequence was selected as the targeting moiety (Figure 6A); this approach has been previously explored with other FPP analogues.<sup>24,26</sup> The D1 DARPin was prenylated with C10NorOPP (D1-Nor, 18), followed by conjugation with TAMRA-tetrazine, 13, to generate the D1-TAMRA conjugate (19), whose identity was confirmed using LC-MS (Figure S8). D1-TAMRA was shown to specifically label EpCAM<sup>+</sup> MCF-7 cells in flow cytometry experiments, and that labeling could be

completely competed away using excess unmodified D1 protein (17) (Figure 6B,C).

In related fluorescence microscopy imaging experiments, D1-TAMRA was shown to specifically target and label the cell surface of EpCAM<sup>+</sup> MCF-7 cells at 4 °C (Figure 6D, upper left), while a control conjugate prepared using a nontargeting E3\_5\_CVIA DARPin<sup>46</sup> (D4-TAMRA) failed to label the MCF-7 cell surface (Figure 6D). Additionally, when the MCF-7 cells were preincubated with a 50-fold excess of unmodified D1 (17), the binding of D1-TAMRA to the cells was completely blocked (Figure 4D, lower left). Interestingly, at 37 °C, D1-TAMRA was efficiently internalized by the targeted MCF-7 cells, shown by the punctate fluorescence observed within the cells (Figure 4D, upper right). These results clearly demonstrate that a DARPin conjugate prepared using C10NorOPP followed by the iEDDA reaction can be used to deliver a fluorescent molecule into cells and suggest that this approach could be used to deliver other cargos, including imaging agents and anticancer toxins for a variety of applications.

**Combination of SPAAC and iEDDA for the Assembly of a Trimeric DARPin-Containing Construct.** The analysis with the DARPin-TAMRA construct described above showed success in cellular labeling comparable to previous work with other analogues of FPP containing a bioorthogonal function-

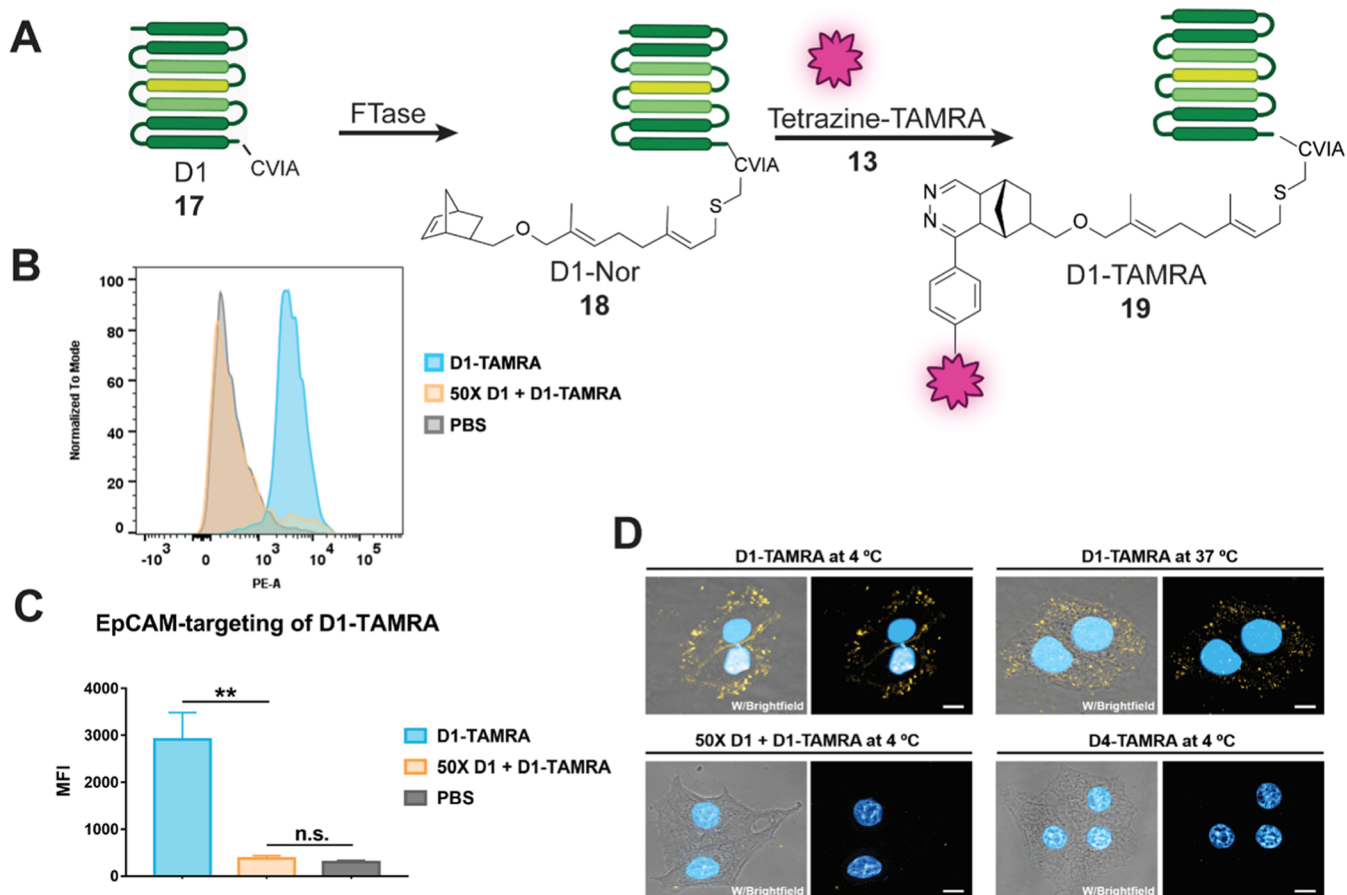


**Figure 6.** Construction of DARPin-TAMRA protein conjugates for targeted cancer cell imaging. (A) Schematic diagram of the preparation of D1-TAMRA (19) using C10NorOPP. The DARPin-CVIA protein was prenylated with C10NorOPP using yFTase, followed by the iEDDEA reaction with TAMRA-tetrazine (13). The anti-EpCAM DARPin-CVIA (D1, 17) protein and nontargeting DARPin-CVIA (D4) protein were used in this study. (B) The D1-TAMRA conjugate was shown to specifically bind to EpCAM-expressing MCF-7 cells by flow cytometry that could be competed with by the inclusion of a 50-fold excess of unlabeled D1. (C) Comparison of the mean fluorescence intensity (MFI) obtained by flow cytometry for binding of D1-TAMRA to MCF-7 cells (via EpCAM) in the absence and presence of competing unlabeled D1. (D) Visualization of the binding (4 °C) and internalization (37 °C) of D1-TAMRA (19) to MCF-7 cells by confocal microscopy (scale bar, 10  $\mu$ m). Non-EpCAM-targeting D4-TAMRA was used as a negative control. D1-TAMRA: yellow; Hoechst 33342 (nucleus): blue; brightfield: gray scale.

ality. However, since C10NorOPP can utilize iEDDA labeling chemistry, it should be possible to combine both iEDDA and SPAAC reactions to form more complex assemblies in a relatively simple manner. To demonstrate this here, a construct containing three DARPin proteins and a TAMRA fluorophore was prepared and used to label EpCAM<sup>+</sup> cells. Starting with a commercially available four-arm poly(ethylene glycol) (4-arm-PEG) polymeric material containing three NHS esters and one azide (4-PEG-NHS<sub>3</sub>-Az, 20), the reaction with tetrazine amine (21) was used to create 4-PEG-Tet<sub>3</sub>-Az (22) (Figure S13). To optimize the attachment of three tetrazine moieties, varying equivalents (3, 4, 6 or 10) of tetrazine amine were used in the reaction (Figure S14A) and the crude reaction mixture was analyzed via reversed-phase high-performance liquid chromatography (RP-HPLC) with UV detection (Figure S14B).

Interestingly, the addition of a large excess of tetrazine amine led to decreased tetrazine substitution, potentially due to a competing side reaction, and hence, the desired 22 was synthesized using only a small excess of tetrazine amine (4 equiv for three sites). Compound 22 was reacted with D1-Nor (18) to yield the 4-PEG-D1<sub>3</sub>-Az (24) construct followed by an SPAAC reaction between the azide and TAMRA-DBCO (23) to yield the desired fluorescently labeled conjugate (25a,

Figure 7A). Size exclusion chromatography was found to be ineffective for the purification process; however, Ni-NTA affinity chromatography proved to be a successful alternative, made possible by the presence of a histidine tag at the N-terminus of D1 (17). A combination of isocratic and gradient elution methods was employed to isolate 4-PEG-D1<sub>3</sub>-TAMRA (25a) as the major component (Figure 7B, lane 4). Following the same cell treatment procedure described above for the monomeric DARPin, MCF-7 cells were treated with the new trimeric construct (25a), leading to efficient binding to EpCAM-expressing cells. The affinity of this new construct was measured via flow cytometry and the  $K_d$  was found to be 7.63 nM (Figures 7C and S16). For comparison, the  $K_d$  for the D1-TAMRA (19) construct was determined to be 3.79 nM. The similarity of these two values indicates that there is no multivalent binding to cellular EpCAM due to the trivalent nature of 25a. That could simply reflect the short length of the PEG arms (12 PEG units) of the construct that may preclude bridging the distance between neighboring EpCAM molecules on the cell surface. Given the modular nature of the overall design, multivalent binding could be addressed using longer PEG arms or by switching to other cell surface protein targets that may be more densely packed. It is also important to note



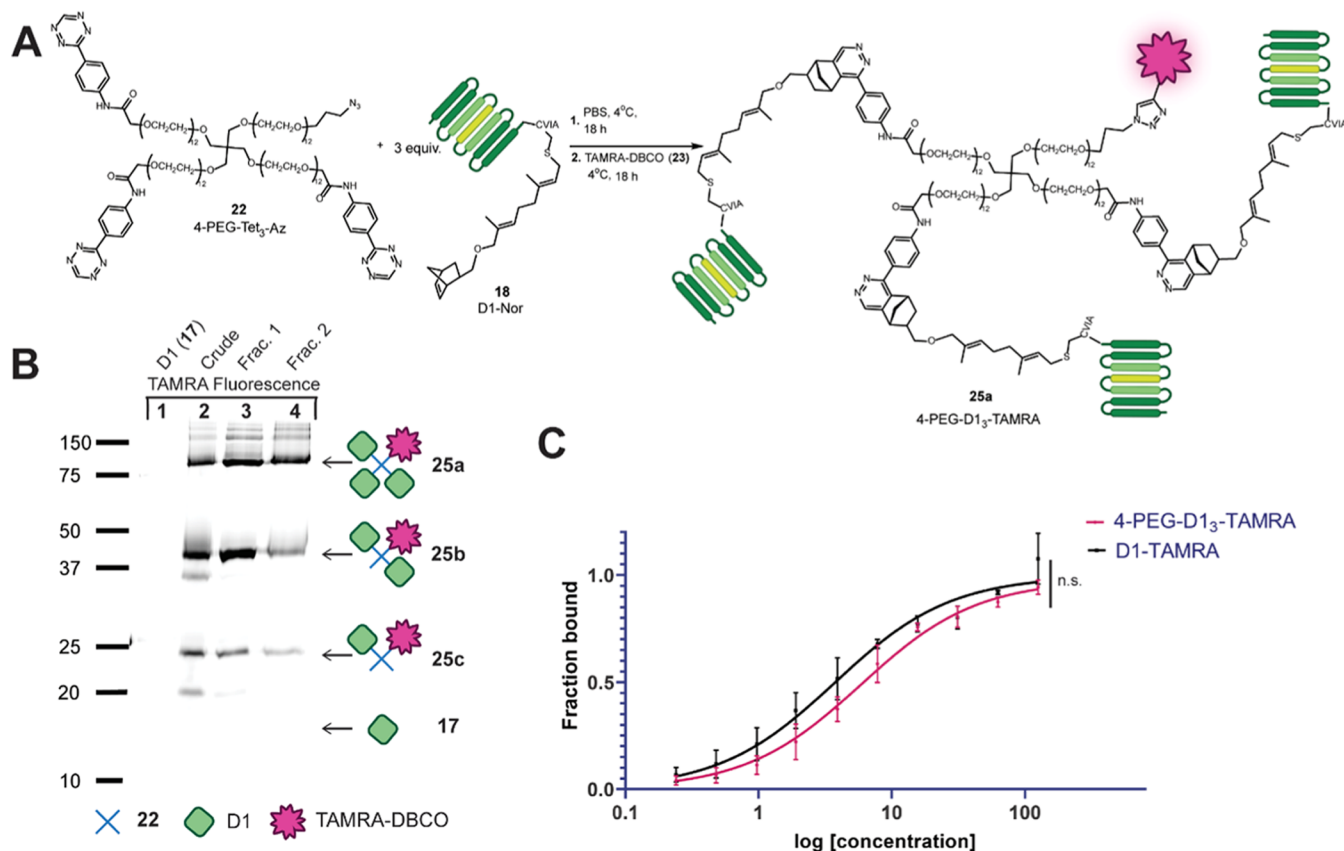


**Figure 7.** Assembly of trimeric DARPIn conjugate and activity analysis. (A) Synthetic scheme for the construction of the 4-PEG-D1<sub>3</sub>-TAMRA (25a) conjugate. (B) Sodium dodecyl sulfate-polyacrylamide gel electrophoresis (SDS-PAGE) analysis of purification of the 4-PEG-D1<sub>3</sub>-TAMRA (25a) conjugate. Left panel: fluorescence scan to visualize TAMRA fluorescence; lane 1: unmodified D1; lane 2: crude reaction mixture after iEDDA ligation and SPAAC reaction. Lane 3: fraction 1 from Ni-NTA purification containing 4-PEG-D1<sub>3</sub>-TAMRA (25a) along with some dimeric and monomeric species; lane 4: fraction 2 from Ni-NTA purification contained mostly 4-PEG-D1<sub>3</sub>-TAMRA (25a) and lesser amounts of dimeric and monomeric species. (C) Affinity titration experiment comparing the binding constants ( $K_d$ ) of 4-PEG-D1<sub>3</sub>-TAMRA and D1-TAMRA to those of MCF-7 cells. Cells were incubated with indicated D1 conjugate 4-PEG-D1<sub>3</sub>-TAMRA (25a) or D1-TAMRA (19) at indicated concentrations (0, 0.24, 0.48, 0.97, 1.9, 3.9, 7.8, 15.6, 31.1, 62.5, 125 nM) for 45 min at 4 °C, and the cells were analyzed via flow cytometry. The results are expressed as the fraction of EpCAM receptors bound with D1 conjugates in 10,000 cells.  $K_d$  values obtained for 4-PEG-D1<sub>3</sub>-TAMRA (25a) and D1-TAMRA (17) are 7.63 and 3.79 nM, respectively. Significance in difference in  $K_d$  value in (C) was tested using a two-tailed, unpaired *t*-test and is indicated as \**P* < 0.1.

that this approach using two distinct bioorthogonal reactions for protein conjugation could be easily adapted for the design of bispecific proteins, an area of intense interest.

Finally, it is worth noting that PEGylation of these DARPins appears to improve their handling when they were subjected to FTase-catalyzed protein modification. Proteins including DARPins modified with hydrophobic isoprenoids sometimes exhibit decreased solubility. For example, in the preparation of D1-TAMRA (19), we observed some precipitation when concentrating this protein via ultrafiltration. In contrast, no precipitation was observed with the trimeric species. Those solubility issues may be, in part, responsible for the greater variation observed in the titration experiment shown in Figure 7C, for 25, particularly at higher concentrations. Overall, these experiments illustrate the enhanced capabilities afforded by having access to two different types of bioorthogonal reactions for the facile assembly of multifunctional protein conjugates. To put this in perspective, while the work reported here is obviously in its infancy, significant progress has been made in the last 10 years in implementing enzymatic methods for protein modification. Several antibody conjugates prepared using such methods have been studied or are currently in

clinical trials, including PF-06664178 (obtained using transglutaminase),<sup>47</sup> ADCT-601 (prepared using glycosyltransferases),<sup>48</sup> Trph-222 (assembled using formylglycine generating enzyme),<sup>49</sup> NBE-002 (created using sortase),<sup>50</sup> and LCB14-0110 (employing farnesyltransferase).<sup>51</sup> Given this plethora of examples, it seems likely that methods such as the one described here that capitalize on multiple degrees of orthogonality will be useful in future generations of bioconjugates.

## CONCLUSIONS

The development of novel bioorthogonal chemical probes is of fundamental utility for studying biological systems. Here, we demonstrate how the norbornene–tetrazine ligation methodology can be used to both study prenylation and develop new approaches for selective protein labeling. To accomplish that, C10NorOPP, an FPP analogue with an ether-linked norbornene functionality, was prepared. *In vitro* kinetic analysis revealed that C10NorOPP is an efficient substrate for FTase with a  $k_{cat}/K_M$  parameter comparable with that of the natural substrate, FPP. Metabolic labeling with C10NorOPP was observed in several cell lines; subsequent proteomic analysis of

proteins enriched via ligation with a tetrazine–biotin reagent identified 24 prenylated proteins in HeLa cells, with farnesylated proteins being the predominant type identified. Those results are consistent with the length of C10NorOPP compared with FPP. Interestingly, while there is overlap with prenylated proteins identified with other related probes, such as C15AlkOPP, several important differences were observed. Potentially, through co-treatment with both probes, a more diverse subset of the prenylation targets could be identified in a single experiment. Additionally, such an approach might be useful for tracking different post-translational modifications, such as prenylation (using norbornene analogues) and palmitoylation (using alkyne analogues), in a simultaneous manner. This is not an entirely novel approach; a multiprobe strategy has been demonstrated in the past utilizing both the Suzuki–Miyaura and CuAAC bioconjugation at the same time from dually labeled cell lysate.<sup>52</sup>

In a different type of application, C10NorOPP was used to enzymatically modify an EpCAM targeting DARPIn in a site-selective manner. Subsequent ligation with a TAMRA-tetrazine reagent allowed EpCAM<sup>+</sup> cells to be targeted and visualized by confocal microscopy and flow cytometry. Finally, the same norbornene-functionalized DARPIn was used to assemble a more complex structure based on a 4-arm PEG core functionalized with three DARPins and a fluorophore. Importantly, the former was linked via iEDA ligation, while the latter was conjugated via SPAAC chemistry. Overall, the development of C10NorOPP and the opportunities enabled by the additional chemical orthogonality afforded by this new reagent have substantially increased the scope and utility of what can be accomplished by using FTase-catalyzed protein labeling.

## ■ ASSOCIATED CONTENT

### Data Availability Statement

The mass spectrometry proteomics data have been deposited to the ProteomeXchange Consortium via the PRIDE partner repository with the data set identifier PXD045277.

### Supporting Information

The Supporting Information is available free of charge at <https://pubs.acs.org/doi/10.1021/acs.bioconjchem.4c00072>.

Figures show kinetic analysis of C10NorOPP, proteomic data analysis, and characterization data for DARPIn conjugates; reaction schemes for *in vitro* prenylation of peptides; methodologies and characterization of synthesized compounds (PDF)

List of prenylated proteins found in with C10NorOPP (Table S1) (XLSX)

Ungrouped Comparisons between proteins found with C10NorOPP and C15AlkOPP (Table S2) (XLSX)

Data used to generate correlation plot Figure 5C (Table S3) (XLSX)

Processed Proteomic Data and Data used to generated ranked plot Figure 5A (Table S4) (XLSX)

## ■ AUTHOR INFORMATION

### Corresponding Author

Mark D. Distefano – Department of Chemistry, University of Minnesota—Twin Cities, Minneapolis, Minnesota 55455, United States; [orcid.org/0000-0002-2872-0259](https://orcid.org/0000-0002-2872-0259); Email: [diste001@umn.edu](mailto:diste001@umn.edu)

## Authors

Shelby A. Auger – Department of Chemistry, University of Minnesota—Twin Cities, Minneapolis, Minnesota 55455, United States; [orcid.org/0000-0003-2873-2580](https://orcid.org/0000-0003-2873-2580)

Sneha Venkatachalapathy – Department of Chemistry, University of Minnesota—Twin Cities, Minneapolis, Minnesota 55455, United States

Kiall Francis G. Suazo – Department of Chemistry, University of Minnesota—Twin Cities, Minneapolis, Minnesota 55455, United States; [orcid.org/0000-0002-0803-8332](https://orcid.org/0000-0002-0803-8332)

Yiao Wang – Department of Chemistry, University of Minnesota—Twin Cities, Minneapolis, Minnesota 55455, United States; [orcid.org/0000-0002-0229-5768](https://orcid.org/0000-0002-0229-5768)

Alexander W. Sarkis – Department of Chemistry, University of Minnesota—Twin Cities, Minneapolis, Minnesota 55455, United States

Kaitlyn Bernhagen – Department of Chemistry, University of Minnesota—Twin Cities, Minneapolis, Minnesota 55455, United States

Katarzyna Justyna – Department of Chemistry, University of Minnesota—Twin Cities, Minneapolis, Minnesota 55455, United States

Jonas V. Schaefer – Department of Biochemistry, University of Zurich, Zurich CH-8057, Switzerland

James W. Wollack – Department of Chemistry and Biochemistry, St. Catherine University, St. Paul, Minnesota 55105, United States; [orcid.org/0000-0003-3124-721X](https://orcid.org/0000-0003-3124-721X)

Andreas Plückthun – Department of Biochemistry, University of Zurich, Zurich CH-8057, Switzerland; [orcid.org/0000-0003-4191-5306](https://orcid.org/0000-0003-4191-5306)

Ling Li – Department of Experimental and Clinical Pharmacology, University of Minnesota—Twin Cities, Minneapolis, Minnesota 55455, United States

Complete contact information is available at:

<https://pubs.acs.org/10.1021/acs.bioconjchem.4c00072>

## Author Contributions

S.A.A. wrote the manuscript. S.A.A., A.W.S., K.F.G.S., K.B., Y.W., J.W.W., S.V., and K.J. all conducted experiments and interpreted data. S.A.A., K.J., and J.W.W. generated and developed a methodology to synthesize compounds. A.W.S. and J.W.W. determined kinetic parameters. K.F.G.S. and S.A.A. did proteomic analysis and data interpretation. K.F.G.S. and S.A.A. did metabolic labeling. Y.W. constructed protein-conjugate and did *in cellulo* imaging. S.V. constructed and developed trimer conjugate. M.D.D., J.W.W., L.L., J.S., and A.P. assisted in the experimental design, supervised work on the project, and edited the manuscript.

## Notes

The authors declare no competing financial interest.

## ■ ACKNOWLEDGMENTS

The authors acknowledge Drs. Yingchun Zhao and Peter Villalta for the assistance with proteomic data collection in the Analytical Biochemistry Shared Resource of the Masonic Cancer Center, designated by the National Cancer Institute and supported by P30 CA077598. This work was supported by the resources and staff at the University of Minnesota University Imaging Centers (UIC). SCR\_020997. K.F.G.S. was supported by a Doctoral Dissertation Fellowship from the University of Minnesota. S.A.A. was supported by the National Science Foundation Grant CHE-1851990, the National

Institutes of Health Training under Grants T32 GM132029 and T32 AG029796 and by a Doctoral Dissertation Fellowship from the University of Minnesota. This work was supported by the National Institute of Health under grants RF1AG056976 (L.L. and M.D.D.) and R35GM141853 (M.D.D.).

## REFERENCES

- (1) Hottman, D. A.; Li, L. Protein Prenylation and Synaptic Plasticity: Implications for Alzheimer's Disease. *Mol. Neurobiol.* **2014**, *50*, 177–185.
- (2) Sebti, S. M. Protein Farnesylation: Implications for Normal Physiology, Malignant Transformation, and Cancer Therapy. *Cancer Cell* **2005**, *7* (4), 297–300.
- (3) Wang, M.; Casey, P. J. Protein Prenylation: Unique Fats Make Their Mark on Biology. *Nat. Rev. Mol. Cell Biol.* **2016**, *17* (2), 110–122.
- (4) Rashidi, S.; Tuteja, R.; Mansouri, R.; Ali-Hassanzadeh, M.; Shafiei, R.; Ghani, E.; Karimazar, M.; Nguewa, P.; Manzano-Román, R. The Main Post-Translational Modifications and Related Regulatory Pathways in the Malaria Parasite *Plasmodium Falciparum*: An Update. *J. Proteomics* **2021**, *245*, No. 104279.
- (5) Qu, W.; Suazo, K. F.; Liu, W.; Cheng, S.; Jeong, A.; Hottman, D.; Yuan, L. L.; Distefano, M. D.; Li, L. Neuronal Protein Farnesylation Regulates Hippocampal Synaptic Plasticity and Cognitive Function. *Mol. Neurobiol.* **2021**, *58* (3), 1128–1144.
- (6) Li, H.; Kuwajima, T.; Oakley, D.; Nikulina, E.; Hou, J.; Yang, W. S.; Lowry, E. R.; Lamas, N. J.; Amoroso, M. W.; Croft, G. F.; Hosur, R.; Wichterle, H.; Sebti, S.; Filbin, M. T.; Stockwell, B.; Henderson, C. E. Protein Prenylation Constitutes an Endogenous Brake on Axonal Growth. *Cell Rep.* **2016**, *16* (2), 545–558.
- (7) Palsuledesai, C. C.; Distefano, M. D. Protein Prenylation: Enzymes, Therapeutics, and Biotechnology Applications. *ACS Chem. Biol.* **2015**, *10*, 51–62.
- (8) Kuchay, S.; Wang, H.; Marzio, A.; Jain, K.; Homer, H.; Fehrenbacher, N.; Philips, M. R.; Zheng, N.; Pagano, M. GGTase3 Is a Newly Identified Geranylgeranyltransferase Targeting a Ubiquitin Ligase. *Nat. Struct. Mol. Biol.* **2019**, *26* (7), 628–636.
- (9) Shirakawa, R.; Goto-Ito, S.; Goto, K.; Wakayama, S.; Kubo, H.; Sakata, N.; Trinh, D. A.; Yamagata, A.; Sato, Y.; Masumoto, H.; Cheng, J.; Fujimoto, T.; Fukai, S.; Horiuchi, H. A SNARE Geranylgeranyltransferase Essential for the Organization of the Golgi Apparatus. *EMBO J.* **2020**, *39* (8), No. e104120, DOI: 10.15252/embj.2019104120.
- (10) Suazo, K. F.; Park, K.-Y.; Distefano, M. D. A Not-So-Ancient Grease History: Click Chemistry and Protein Lipid Modifications. *Chem. Rev.* **2021**, *121* (12), 7178–7248.
- (11) Berry, A. F. H.; Heal, W. P.; Tarafder, A. K.; Tolmachova, T.; Baron, R. A.; Seabra, M. C.; Tate, E. W. Rapid Multilabel Detection of Geranylgeranylated Proteins by Using Bioorthogonal Ligation Chemistry. *ChemBioChem* **2010**, *11* (6), 771–773.
- (12) Wang, Y. C.; Distefano, M. D. Synthetic Isoprenoid Analogues for the Study of Prenylated Proteins: Fluorescent Imaging and Proteomic Applications. *Bioorg. Chem.* **2016**, *64*, 59–65.
- (13) Turek-Etienne, T. C.; Strickland, C. L.; Distefano, M. D. Biochemical and Structural Studies with Prenyl Diphosphate Analogues Provide Insights into Isoprenoid Recognition by Protein Farnesyl Transferase. *Biochemistry* **2003**, *42* (13), 3716–3724.
- (14) Suazo, K. F.; Jeong, A.; Ahmadi, M.; Brown, C.; Qu, W.; Li, L.; Distefano, M. D. Metabolic Labeling with an Alkyne Probe Reveals Similarities and Differences in the Prenylomes of Several Brain-Derived Cell Lines and Primary Cells. *Sci. Rep.* **2021**, *11* (1), No. 4367.
- (15) Storck, E. M.; Morales-Sanfrutos, J.; Serwa, R. A.; Panyain, N.; Lanyon-Hogg, T.; Tolmachova, T.; Ventimiglia, L. N.; Martin-Serrano, J.; Seabra, M. C.; Wojciak-Stothard, B.; Tate, E. W. Dual Chemical Probes Enable Quantitative System-Wide Analysis of Protein Prenylation and Prenylation Dynamics. *Nat. Chem.* **2019**, *11* (6), 552–561.
- (16) Ravasco, J. M. J. M.; Monteiro, C. M.; Trindade, A. F. Cyclopropenes: A New Tool for the Study of Biological Systems. *Org. Chem. Front.* **2017**, *4* (6), 1167–1198.
- (17) Patterson, D. M.; Nazarova, L. A.; Xie, B.; Kamber, D. N.; Prescher, J. A. Functionalized Cyclopropenes as Bioorthogonal Chemical Reporters. *J. Am. Chem. Soc.* **2012**, *134* (45), 18638–18643.
- (18) Handula, M.; Chen, K.-T.; Seimille, Y. IEDDA: An Attractive Bioorthogonal Reaction for Biomedical Applications. *Molecules* **2021**, *26* (15), No. 4640, DOI: 10.3390/MOLECULES26154640.
- (19) Devaraj, N. K.; Hilderbrand, S.; Upadhyay, R.; Mazitschek, R.; Weissleder, R. Bioorthogonal Turn-On Probes for Imaging Small Molecules inside Living Cells. *Angew. Chem., Int. Ed.* **2010**, *49* (16), 2869–2872.
- (20) Wollack, J. W.; Monson, B. J.; Dozier, J. K.; Dalluge, J. J.; Poss, K.; Hilderbrand, S. A.; Distefano, M. D. Site-Specific Labeling of Proteins and Peptides with Trans-Cyclooctene Containing Handles Capable of Tetrazine Ligation. *Chem. Biol. Drug Des.* **2014**, *84* (2), 140–147.
- (21) Vrabel, M.; Kölle, P.; Brunner, K. M.; Gattner, M. J.; López-Carrillo, V.; de Vivie-Riedle, R.; Carell, T. Norbornenes in Inverse Electron-Demand Diels-Alder Reactions. *Chem.—Eur. J.* **2013**, *19* (40), 13309–13312.
- (22) Suazo, K. F.; Schaber, C.; Palsuledesai, C. C.; John, A. R. O.; Distefano, M. D. Global Proteomic Analysis of Prenylated Proteins in *Plasmodium Falciparum* Using an Alkyne-Modified Isoprenoid Analogue. *Sci. Rep.* **2016**, *6*, No. 38615, DOI: 10.1038/srep38615.
- (23) Lastra, A. L. D. L.; Hassan, S.; Tate, E. W. Deconvoluting the Biology and Druggability of Protein Lipidation Using Chemical Proteomics. *Curr. Opin. Chem. Biol.* **2020**, *2021*, 97–112.
- (24) Zhang, Y.; Auger, S.; Schaefer, J. V.; Plückthun, A.; Distefano, M. D. Site-Selective Enzymatic Labeling of Designed Ankyrin Repeat Proteins Using Protein Farnesyltransferase. In *Bioconjugation*; Massa, S.; Devoogdt, N., Eds.; Methods in Molecular Biology; Humana: New York, 2019; Vol. 2033, pp 207–219.
- (25) Wang, Y.; Kilic, O.; Csizmar, C. M.; Ashok, S.; Hougland, J. L.; Distefano, M. D.; Wagner, C. R. Engineering Reversible Cell–Cell Interactions Using Enzymatically Lipidated Chemically Self-Assembled Nanorings. *Chem. Sci.* **2021**, *12* (1), 331–340.
- (26) Zhang, Y.; Wang, Y.; Uslu, S.; Venkatachalapathy, S.; Rashidian, M.; Schaefer, J. V.; Plückthun, A.; Distefano, M. D. Enzymatic Construction of DARPIn-Based Targeted Delivery Systems Using Protein Farnesyltransferase and a Capture and Release Strategy. *Int. J. Mol. Sci.* **2022**, *23* (19), No. 11537, DOI: 10.3390/ijms231911537.
- (27) Khongorzul, P.; Ling, C. J.; Khan, F. U.; Ihsan, A. U.; Zhang, J. Antibody–Drug Conjugates: A Comprehensive Review. *Mol. Cancer Res.* **2020**, *18* (1), 3–19.
- (28) Beck, A.; Goetsch, L.; Dumontet, C.; Corvaia, N. Strategies and Challenges for the next Generation of Antibody–Drug Conjugates. *Nat. Rev. Drug Discovery* **2017**, *16* (5), 315–337.
- (29) Merten, H.; Brandl, F.; Plückthun, A.; Zangemeister-Wittke, U. Antibody–Drug Conjugates for Tumor Targeting—Novel Conjugation Chemistries and the Promise of Non-IgG Binding Proteins. *Bioconjugate Chem.* **2015**, *26* (11), 2176–2185.
- (30) Zahnd, C.; Kawe, M.; Stumpp, M. T.; de Pasquale, C.; Tamaskovic, R.; Nagy-Davidescu, G.; Dreier, B.; Schibli, R.; Binz, H. K.; Waibel, R.; Plückthun, A. Efficient Tumor Targeting with High-Affinity Designed Ankyrin Repeat Proteins: Effects of Affinity and Molecular Size. *Cancer Res.* **2010**, *70* (4), 1595–1605.
- (31) Plückthun, A. Designed Ankyrin Repeat Proteins (DARPs): Binding Proteins for Research, Diagnostics, and Therapy. *Annu. Rev. Pharmacol. Toxicol.* **2015**, *55* (1), 489–511.
- (32) Knall, A. C.; Hollauf, M.; Slugovc, C. Kinetic Studies of Inverse Electron Demand Diels-Alder Reactions (IEDDA) of Norbornenes and 3,6-Dipyridin-2-Yl-1,2,4,5-Tetrazine. *Tetrahedron Lett.* **2014**, *55* (34), 4763–4766.
- (33) Vervacke, J. S.; Funk, A. L.; Wang, Y. C.; Strom, M.; Hrycyna, C. A.; Distefano, M. D. Diazirine-Containing Photoactivatable Isoprenoid: Synthesis and Application in Studies with Isoprenylcys-

- teine Carboxyl Methyltransferase. *J. Org. Chem.* **2014**, *79* (5), 1971–1978.
- (34) Hosokawa, A.; Wollack, J. W.; Zhang, Z.; Chen, L.; Barany, G.; Distefano, M. D. Evaluation of an Alkyne-Containing Analogue of Farnesyl Diphosphate as a Dual Substrate for Protein-Prenyltransferases. *Int. J. Pept. Res. Ther.* **2007**, *13* (1–2), 345–354.
- (35) DeGraw, A. J.; Palsuledesai, C.; Ochocki, J. D.; Dozier, J. K.; Lenevich, S.; Rashidian, M.; Distefano, M. D. Evaluation of Alkyne-Modified Isoprenoids as Chemical Reporters of Protein Prenylation. *Chem. Biol. Drug Des.* **2010**, *76* (6), 460–471.
- (36) Suazo, K. F.; Hurben, A. K.; Liu, K.; Xu, F.; Thao, P.; Sudheer, C.; Li, L.; Distefano, M. D. Metabolic Labeling of Prenylated Proteins Using Alkyne-Modified Isoprenoid Analogues. *Curr. Protoc. Chem. Biol.* **2018**, *10* (3), No. e46.
- (37) Palsuledesai, C. C.; Ochocki, J. D.; Kuhns, M. M.; Wang, Y.-C.; Warmka, J. K.; Chernick, D. S.; Wattenberg, E. V.; Li, L.; Arriaga, E. A.; Distefano, M. D. Metabolic Labeling with an Alkyne-Modified Isoprenoid Analog Facilitates Imaging and Quantification of the Prenylome in Cells. *ACS Chem. Biol.* **2016**, *11* (10), 2820–2828.
- (38) Fang, Z.; Chowdhury, S. M. Dual-Stage Neutral Loss Tandem Mass Spectrometric Strategy for Confident Identification of Protein Prenylation. *Anal. Chem.* **2021**, *93* (39), 13169–13176.
- (39) Chung, J. A.; Wollack, J. W.; Hovlid, M. L.; Okesli, A.; Chen, Y.; Mueller, J. D.; Distefano, M. D.; Taton, T. A. Purification of Prenylated Proteins by Affinity Chromatography on Cyclodextrin-Modified Agarose. *Anal. Biochem.* **2009**, *386* (1), 1–8.
- (40) Wilkins, J. A.; Kaasik, K.; Chalkley, R. J.; Burlingame, A. L. Characterization of Prenylated C-Terminal Peptides Using a Thiopropyl-Based Capture Technique and LC-MS/MS\*. *Mol. Cell. Proteomics* **2020**, *19* (6), 1005–1016.
- (41) Crooks, G. E.; Hon, G.; Chandonia, J.-M.; Brenner, S. E. WebLogo: A Sequence Logo Generator. *Genome Res.* **2004**, *14* (6), 1188–1190.
- (42) Schneider, T.; Stephens, M. WebLogo—Create Sequence Logos, 2023. <https://weblogo.berkeley.edu/logo.cgi> (accessed Sept 11, 2023).
- (43) Long, S. B.; Casey, P. J.; Beese, L. S. The Basis for K-Ras4B Binding Specificity to Protein Farnesyl-Transferase Revealed by 2 Å Resolution Ternary Complex Structures. *Structure* **2000**, *8* (2), 209–222.
- (44) Jennings, B. C.; Danowitz, A. M.; Wang, Y.-C.; Gibbs, R. A.; Distefano, M. D.; Fierke, C. A. Analogs of Farnesyl Diphosphate Alter CaaX Substrate Specificity and Reactions Rates of Protein Farnesyltransferase. *Bioorg. Med. Chem. Lett.* **2016**, *26* (4), 1333–1336.
- (45) Stefan, N.; Martin-Killias, P.; Wyss-Stoeckle, S.; Honegger, A.; Zangemeister-Wittke, U.; Plückthun, A. DARPins Recognizing the Tumor-Associated Antigen EpCAM Selected by Phage and Ribosome Display and Engineered for Multivalency. *J. Mol. Biol.* **2011**, *413* (4), 826–843.
- (46) Binz, H. K.; Stumpp, M. T.; Forrer, P.; Amstutz, P.; Plückthun, A. Designing Repeat Proteins: Well-Expressed, Soluble and Stable Proteins from Combinatorial Libraries of Consensus Ankyrin Repeat Proteins. *J. Mol. Biol.* **2003**, *332* (2), 489–503.
- (47) Strop, P.; Delaria, K.; Foletti, D.; Witt, J. M.; Hasa-Moreno, A.; Poulsen, K.; Casas, M. G.; Dorywalska, M.; Farias, S.; Pios, A.; Lui, V.; Dushin, R.; Zhou, D.; Navaratnam, T.; Tran, T.-T.; Sutton, J.; Lindquist, K. C.; Han, B.; Liu, S.-H.; Shelton, D. L.; Pons, J.; Rajpal, A. Site-Specific Conjugation Improves Therapeutic Index of Antibody Drug Conjugates with High Drug Loading. *Nat. Biotechnol.* **2015**, *33* (7), 694–696.
- (48) van Geel, R.; Wijdeven, M. A.; Heesbeen, R.; Verkade, J. M. M.; Wasiel, A. A.; van Berkel, S. S.; van Delft, F. L. Chemoenzymatic Conjugation of Toxic Payloads to the Globally Conserved N-Glycan of Native mAbs Provides Homogeneous and Highly Efficacious Antibody–Drug Conjugates. *Bioconjugate Chem.* **2015**, *26* (11), 2233–2242.
- (49) Maclaren, A.; Levin, N.; Lowman, H.; Trikha, M. Trph-222, a Novel Anti-CD22 Antibody Drug Conjugate (ADC), Has Significant

Anti-Tumor Activity in NHL Xenografts and Is Well Tolerated in Non-Human Primates. *Blood* **2017**, *130* (Suppl. 1), 4105.

(50) Stefan, N.; Gébleux, R.; Waldmeier, L.; Hell, T.; Escher, M.; Wolter, F. I.; Grawunder, U.; Beerli, R. R. Highly Potent, Anthracycline-Based Antibody–Drug Conjugates Generated by Enzymatic, Site-Specific Conjugation. *Mol. Cancer Ther.* **2017**, *16* (5), 879–892.

(51) Lee, J.-J.; Choi, H.-J.; Yun, M.; Kang, Y.; Jung, J.-E.; Ryu, Y.; Kim, T. Y.; Cha, Y.-J.; Cho, H.-S.; Min, J.-J.; Chung, C.-W.; Kim, H.-S. Enzymatic Prenylation and Oxime Ligation for the Synthesis of Stable and Homogeneous Protein–Drug Conjugates for Targeted Therapy. *Angew. Chem., Int. Ed.* **2015**, *54* (41), 12020–12024.

(52) Cao, J.; Boatner, L. M.; Desai, H. S.; Burton, N. R.; Armenta, E.; Chan, N. J.; Castellón, J. O.; Backus, K. M. Multiplexed CuAAC Suzuki–Miyaura Labeling for Tandem Activity-Based Chemo-proteomic Profiling. *Anal. Chem.* **2021**, *93* (4), 2610–2618.